compounds 5 and 6 can be traced down to donor/acceptor interactions that take place in each moiety.

Conclusion

β measurements, using the EFISH technique, provide evidence that the trimethylsilyl group can behave both as a donor and as an acceptor group but more efficiently as a donor group. The back-donation process involved in the Si/donor interaction does not contribute to a significant enhancement of β. The efficiency of the trimethylsilyl group as an electron-releasing group is ascribed to $\sigma-\pi$ interaction. It is found, however, to be less effective than a donor group containing a filled p orbital.

Silicon has also been investigated as part of a conjunction path connecting phenyl rings. The nonplanar geometry of the phenyl-Si-phenyl system prevents silicon from behaving as an efficient transmitter. The additive behavior of β indicates that silicon must not be viewed as an electron bridge connecting conjugated systems. The charge-transfer interactions contributing to the β nonlinearity are confined within each moiety, and the overall nonlinearity can be accordingly accounted for by a vectorially additive model.

Registry No. 1, 16087-24-4; 2, 136155-28-7; 3, 129620-60-6; 4, 129620-64-0; 5, 130104-06-2; 6, 130104-05-1; 7, 18236-77-6; 8, 129620-58-2; 9, 129620-59-3; 10, 129620-61-7; 11, 129620-62-8; 12, 129620-63-9; 13, 18089-97-9; 14, 136155-29-8; 15, 136155-30-1; 16, 18141-19-0; 17, 136155-31-2; 18, 136155-32-3.

Supplementary Material Available: A listing of structure factors (4 pages). Ordering information is given on any current masthead page.

Metal to Ligand Charge-Transfer Photochemistry of Metal–Metal-Bonded Complexes. 10.† Photochemical and Electrochemical Study of the Electron-Transfer Reactions of $Mn(CO)_3(\alpha\text{-diimine})(L)^\cdot$ (L = N-, P-Donor) Radicals Formed by Irradiation of $(CO)_5MnMn(CO)_3(\alpha\text{-diimine})$ Complexes in the Presence of L

T. van der Graaf,‡ R. M. J. Hofstra, P. G. M. Schilder, M. Rijkhoff, and D. J. Stufkens*

Anorganisch Chemisch Laboratorium, J. H. van't Hoff Instituut, Universiteit van Amsterdam, Nieuwe Achtergracht 166, 1018 WV Amsterdam, The Netherlands

J. G. M. van der Linden*

Laboratorium voor Anorganische Chemie, Katholieke Universiteit Nijmegen, Toernooiveld, 6525 ED Nijmegen, The Netherlands

Received January 7, 1991

This article describes the catalytic properties of $Mn(CO)_3(\alpha\text{-diimine})(L)^\cdot$ radicals, formed by irradiation with visible light of the complexes $(CO)_5MnMn(CO)_3(\alpha\text{-diimine})$ (1) in the presence of L (L = N-, P-donor). The radicals initiate the catalytic disproportionation of complexes 1 in an electron transfer chain (ETC) reaction to give $Mn(CO)_5^-$ and $[Mn(CO)_3(\alpha\text{-diimine})(L)]^+$. The efficiency of this reaction is low if L is a hard base; it increases for ligands having smaller cone angles and, for phosphines, higher basicities. The $Mn(CO)_3(\alpha\text{-diimine})(L)^\cdot$ radicals also reduce several of the cluster compounds $M_3(CO)_{12-x}(PR_3)_x$ (M = Fe, Ru; x = 0–2) and catalyze the substitution of CO by PR_3. In that case the efficiency of the reaction is mainly determined by the reduction potentials of the $[Mn(CO)_3(\alpha\text{-diimine})(PR_3)]^+$ cation and the cluster. These potentials have been measured with cyclic voltammetry and differential pulse voltammetry.

Introduction

Many mechanistic studies have been carried out on ligand substitution reactions of metal carbonyls, complexes which play an important role in various catalytic processes.[1] For many years such reactions have been assumed to proceed exclusively via intermediates with 16 or 18 valence electrons. Recently, however, several substitution reactions have been found to proceed much more rapidly via 17- or 19-valence-electron intermediates. Kochi[2] was the first who recognized the important role played by radicals in organometallic chemistry. Since his first publications on this subject many review articles have appeared in which the generation and the structural, spectroscopic, and chemical properties of such radicals are discussed.[3] Odd-electron organometallic species can be

† Part 9: ref 50.

‡ Present address: AKZO Research Laboratories Arnhem, P.O. Box 9300, 6800 SB Arnhem, The Netherlands.

(1) (a) *Organic Synthesis via Metal Carbonyls*; Wender, I., Pino, P., Eds.; Wiley: New York, 1968; Vol. 2. (b) Sheldon, R. A. *Chemicals from Synthesis Gas*; Reidel: Dordrecht, The Netherlands, 1983. (c) *Photocatalysis, Fundamentals and Applications*; Serpone, N. Pelizzetti, E., Eds.; Wiley: New York, 1989.

(2) (a) Kochi, J. K. *Organometallic Mechanisms and Catalysis*; Academic Press: New York, 1978. (b) Kochi, J. K. *J. Organomet. Chem.* 1986, *300*, 139.

0276-7333/91/2310-3668$02.50/0

generated electrochemically or photochemically, and in this article we report the catalytic properties of a special group of radicals that can be generated in both ways. The photoproduction of organometallic radicals normally proceeds by irradiation of metal–metal-bonded species.[3,4] In this way metal-centered radicals such as $M(CO)_5$ (M = Mn, Re), $CpM'(CO)_3$ (M' = Mo, W), $CpFe(CO)_2$, and $Co(CO)_4$ could be identified as transients with time-resolved spectroscopy[5] or as persistent radicals in solution or low-temperature matrices.[6] The substitution reactions of these 17-electron species appeared to proceed associatively with formation of 19-electron intermediates. Such 19-electron radicals are normally short-lived because of their high reducing power and their thermal instability if the odd electron occupies a M–L antibonding orbital. Only a few of these radicals have therefore been observed spectroscopically.[7] The stability of these carbonyl radicals can be enhanced by substitution of two CO ligands by a chelating heteroolefinic molecule such as an *o*-quinone or α-diimine. The odd electron then moves to the low-lying π* orbital of the chelate. Examples of such ligand-localized radicals are $Co(CO)_3$(2,3-bis(diphenylphosphino)maleic anhydride),[8] $Re(CO)_4$(3,5-di-*tert*-butyl-*o*-benzosemiquinone),[9] and $M(CO)_3$(α-diimine)$(PR_3)^\bullet$ (M = Mn, Re).[10]

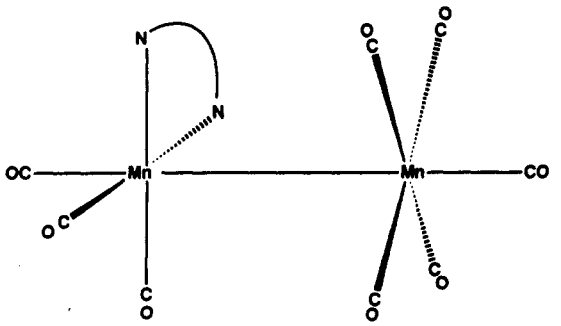

1

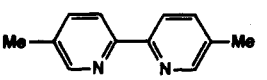

bpy'

a

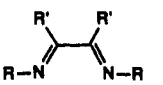

R-DAB[R',R']

b R= iPr, R'=H

b' R= pAn, R'=H

b'' R= pAn, R'=Me

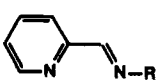

R-PyCa

c R= iPr

Figure 1. General structure of complexes 1 (N⌒N = α-diimine) and of the α-diimine ligands used.

They are in fact 18-electron species in contrast to the 19-electron, metal centered radicals from which they are derived. Due to the presence of an odd electron in an unfavorable orbital these radicals act as reducing species and initiate electron transfer chain (ETC) reactions. ETC catalysis is based on the observation that catalytic amounts of oxidizing or reducing agents considerably increase the rate of a reaction.[3a–c,h,i] Especially, ligand substitution reactions appeared to proceed much more easily in the presence of such agents or by passing a small cathodic or anodic current through the solution.[2] $Mn(CO)_3$(α-diimine)$^\bullet$ radicals are formed by irradiation of the metal–metal-bonded complexes $XMn(CO)_3$(α-diimine) (X = $(CO)_5Mn$, $(CO)_4Co$, $Cp(CO)_2Fe$, and Ph_3Sn).[10] This article describes in detail the ETC reactions induced by $Mn(CO)_3$(α-diimine)(L)$^\bullet$ (L = N-, P-donor) radicals formed by irradiation of $(CO)_5MnMn(CO)_3$(α-diimine) (1) in the presence of excess L. The general structure of complexes 1 is shown in Figure 1. This figure also depicts the structures of the α-diimine ligands used, viz. 4,4'-dimethyl-2,2'-bipyridine (bpy', **a**), 1,4-diaza-1,3-butadiene (R-DAB[R',R'], denoted as R-DAB for R' = H: R = iPr, R' = H (**b**); R = pAn (=*p*-anisyl), R' = H (**b'**); R = pAn, R' = Me (**b''**); and pyridine-2-carbaldehyde isopropylimine (iPr-PyCa, **c**)).

The complexes all possess a $\sigma_b \rightarrow \sigma^*$ transition of the metal–metal bond in the near-UV region and metal to α-diimine charge transfer (MLCT) transitions in the visible

(3) (a) Chanon, M.; Tobe, M. L. *Angew. Chem., Int. Ed. Engl.* **1982**, *21*, 1. (b) Julliard, M.; Chanon, M. *Chem. Rev.* **1983**, *83*, 425. (c) Kaim, W. *Acc. Chem. Res.* **1985**, *18*, 160. (d) Stiegman, A. E.; Tyler, D. R. *Comments Inorg. Chem.* **1986**, *5*, 215. (e) Astruc, D. *Chem. Rev.* **1988**, *88*, 1189. (f) Baird, M. C. *Chem. Rev.* **1988**, *88*, 1217. (g) Tyler, D. R. *Prog. Inorg. Chem.* **1988**, *36*, 125. (h) Astruc, D. *Angew. Chem., Int. Ed. Engl.* **1988**, *27*, 643. (i) Kochi, J. K. *Angew. Chem., Int. Ed. Engl.* **1988**, *27*, 1227. (j) *Paramagnetic Organometallic Species in Activation, Selectivity, Catalysis*; Chanon, M., Julliard, M., Poite, J. C., Eds.; NATO ASI Series C; Kluwer Academic: Dordrecht, The Netherlands, 1988; Vol. 257. (k) Tyler, D. R. In *Organometallic Radical Processes*; Journal of Organometallic Chemistry Library 22, Trogler, W. C., Ed.; Elsevier: Amsterdam, 1990; p 338.

(4) (a) Geoffroy, G. L.; Wrighton, M. S. *Organometallic Photochemistry*; Academic Press: New York, 1979. (b) Stiegman, A. E.; Tyler, D. R. *Acc. Chem. Res.* **1984**, *17*, 61. (c) Meyer, T. J.; Caspar, J. V. *Chem. Rev.* **1985**, *85*, 187. (d) Stiegman, A. E.; Tyler, D. R. *Coord. Chem. Rev.* **1985**, *63*, 217. (e) Stufkens, D. J. In *Stereochemistry of Organometallic and Inorganic Compounds*; Bernal, I., Ed.; Elsevier: Amsterdam, 1989; Vol. 3, p 226. (f) Tyler, D. R.; Mao, F. *Coord. Chem. Rev.* **1990**, *97*, 119.

(5) (a) Yesaka, H.; Kobayashi, T.; Yasufuku, K.; Nagakura, S. *J. Am. Chem. Soc.* **1983**, *105*, 6249. (b) Kobayashi, T.; Ohtani, H.; Noda, H.; Teratani, S.; Yamazaki, H.; Yasufuku, K. *Organometallics* **1986**, *5*, 110. (c) Rothberg, L. J.; Cooper, N. J.; Peter, K. S.; Vaida, V. *J. Am. Chem. Soc.* **1982**, *104*, 3536. (d) Hughey, C. J. L., IV; Anderson, C. P.; Meyer, Th. J. *J. Organomet. Chem.* **1977**, *125*, C49. (e) Herrick, R. S.; Herrinton, T. R.; Walker, H. W.; Brown, T. L. *Organometallics* **1985**, *4*, 42. (f) Hanckel, J. M.; Lee, K.; Rushman, P.; Brown, T. L. *Inorg. Chem.* **1986**, *25*, 1852. (g) Rushman, P.; Brown, T. L. *J. Am. Chem. Soc.* **1987**, *109*, 3632. (h) Freedman, A.; Bersohn, R. *J. Am. Chem. Soc.* **1978**, *100*, 4116. (i) Bray, R. G.; Seidler, P. F., Jr.; Gethner, J. S.; Woodin, R. L. *J. Am. Chem. Soc.* **1986**, *108*, 1312. (j) Seder, T. A.; Church, S. P.; Weitz, E. *J. Am. Chem. Soc.* **1986**, *108*, 7518. (k) Poliakoff, M.; Weitz, E. *Adv. Organomet. Chem.* **1986**, *25*, 277. (l) Moore, B. D.; Simpson, M. B.; Poliakoff, M.; Turner, J. J. *J. Chem. Soc., Chem. Commun.* **1984**, 785. (m) Moore, B. D.; Poliakoff, M.; Turner, J. J. *J. Am. Chem. Soc.* **1986**, *108*, 1819. (n) Waltz, W. L.; Hackelberg, O.; Dorfman, L. M.; Wojcicki, A. *J. Am. Chem. Soc.* **1978**, *100*, 7259. (o) Meckstroth, W. K.; Walters, R. T.; Waltz, W. L.; Wojcicki, A.; Dorfman, L. M. *J. Am. Chem. Soc.* **1982**, *104*, 1842. (p) Junk, G. A.; Svec, H. J. *J. Chem. Soc. A* **1970**, 2102.

(6) (a) Church, S. P.; Poliakoff, M.; Timney, J. A.; Turner, J. J. *J. Am. Chem. Soc.* **1981**, *103*, 7515. (b) Sijmons, M. C. R.; Sweany, R. L. *Organometallics* **1982**, *1*, 834. (c) Huber, H.; Kundig, E. P.; Ozin, G. A. *J. Am. Chem. Soc.* **1974**, *96*, 5585. (d) Kidd, D. R.; Cheng, C. P.; Brown, T. L. *J. Am. Chem. Soc.* **1978**, *100*, 4103. (e) McCullen, S. B.; Walker, H. K.; Brown, T. L. *J. Am. Chem. Soc.* **1982**, *104*, 4007. (f) McCullen, S. B.; Brown, T. L. *J. Am. Chem. Soc.* **1982**, *104*, 7496. (g) Walker, H. W.; Rattinger, G. B.; Belford, R. L.; Brown, T. L. *Organometallics* **1983**, *2*, 775. (h) Tyler, D. R.; Goldman, A. S. *J. Organomet. Chem.* **1986**, *311*, 349.

(7) (a) Anderson, O. P.; Sijmons, M. C. R. *J. Chem. Soc., Chem. Commun.* **1972**, 1020. (b) Lionel, T.; Morton, J. R.; Preston, K. F. *Chem. Phys. Lett.* **1981**, *81*, 17. (c) Maroney, M. J.; Trogler, W. C. *J. Am. Chem. Soc.* **1984**, *106*, 4144.

(8) Mao, F.; Tyler, D. R.; Keszler, D. *J. Am. Chem. Soc.* **1989**, *111*, 130.

(9) (a) Creber, K. A. M.; Wan, J. K. S. *J. Am. Chem. Soc.* **1981**, *103*, 2101. (b) Creber, K. A. M.; Wan, J. K. S. *Can. J. Chem.* **1983**, *61*, 1017.

(10) Stufkens, D. J. *Coord. Chem. Rev.* **1990**, *104*, 39.

region. Irradiation into either of these transitions leads to efficient homolysis of the metal–metal bond with $\phi > 0.4$ (eq 1). In the absence of a coordinating ligand or

$$1 \xrightarrow{h\nu} {}^{\bullet}Mn(CO)_5 + Mn(CO)_3(\alpha\text{-diimine})^{\bullet} \quad (1)$$

solvent the 16e $Mn(CO)_3(\alpha$-diimine)$^{\bullet}$ radicals dimerize to give $Mn_2(CO)_6(\alpha\text{-diimine})_2$ (2). In the presence of N- or P-donor ligands L, $Mn(CO)_3(\alpha$-diimine)(L)$^{\bullet}$ radical adducts are formed, which have been identified with ESR,[11] and which have been shown to initiate the catalytic disproportionation of the parent complex according to reaction 2.[12] Similar photodisproportionation reactions have

$$Mn(CO)_3(\alpha\text{-diimine})(L)^{\bullet} + 1 \rightarrow [Mn(CO)_3(\alpha\text{-diimine})(L)]^{+} + [(CO)_5MnMn(CO)_3(\alpha\text{-diimine})]^{-} \quad (2)$$

been observed for other metal–metal-bonded complexes, e.g. for $Cp_2Mo_2(CO)_6$ in the presence of PR_3 (reaction 3).[13]

$$CpMo(CO)_3(PR_3)^{\bullet} + Cp_2Mo_2(CO)_6 \rightarrow [CpMo(CO)_3(PR_3)]^{+} + [Cp_2Mo_2(CO)_6]^{-} \quad (3)$$

In this article we report the factors determining the efficiency of reaction 2 and of the ETC reactions between $Mn(CO)_3(\alpha$-diimine)(L)$^{\bullet}$ radicals and several $M_3(CO)_{12-x}(PR_3)_x$ (M = Fe, Ru, Os; x = 0–2) clusters.

In order to establish the driving force for these electron-transfer reactions, the redox potentials of the various donors and acceptors have been measured with cyclic and differential pulse voltammetry.

Experimental Section

Materials and Preparations. THF, 2-MeTHF, and toluene were dried by distillation from sodium wire under N_2 and stored in Schlenk flasks under N_2. Tetrabutylammonium hexafluorophosphate (TBAH; Hicol), silver trifluoromethanesulfonate (Ag(OTf); Aldrich), $Mn_2(CO)_{10}$ (Strem), $Ru_3(CO)_{12}$ (Strem), $Os_3(CO)_{12}$ (Strem), and bpy′ (Aldrich) were used as received. iPr-PyCa and R-DAB ligands were synthesized according to literature procedures.[14] The complexes **1a–c**[15] and $M_3(CO)_{12-x}(PR_3)_x$ (M = Fe, Ru; x = 0–3)[16] were synthesized according to literature methods. $[Mn(CO)_3(\alpha$-diimine)(L)][OTf] (L = py, PR_3) were prepared by addition of 1 equiv of L to a THF solution of $[Mn(CO)_3(\alpha$-diimine)(THF)][OTf].[12]

Spectroscopy and Photochemistry. IR spectra were recorded on a Nicolet 7199B FTIR spectrometer using a broad-band MCT detector. Electronic absorption spectra were recorded on a Perkin-Elmer Lambda 5 UV/vis spectrometer connected to a Perkin-Elmer 3600 Data Station. The 514.5-nm line of a Spectra-Physics 2025 argon ion laser was used for the quantum yield determinations. A Philips HPK 125-W mercury lamp filtered with a 546-nm interference filter was used in all other irradiations (unless stated otherwise). The compositions of the sample solutions represent the molar ratios of the components, the value 1 corresponding to a concentration of approximately 10^{-2} M for IR samples and of approximately 10^{-4} M for UV/vis samples.

In order to study the influence of the PR_3 ligand on the rate of the photodisproportionation of the complexes, the very light sensitive **1a**/PR_3 (1:50) solutions were prepared in a carefully blinded, red light illuminated room. IR and UV/vis samples were then placed in a specially constructed black box equipped with shutters that allowed the recording of the spectra but prevented stray light from entering the samples during all handling.

Irradiations of $^1/_{32}$–1 s were executed with a camera shutter that was placed between the sample and the light source. All irradiations and subsequent measurements of the UV/vis samples were performed inside the sample holder of the spectrometer. A laser beam, transmitted via a glass fiber, was used as a light source. The power of the laser light was attenuated by gray filters to approximately 1 mW and focused on the vigorously stirred solution. The photochemically initiated disproportionation was then followed by monitoring the sample absorption decay at a certain wavelength. After each light pulse the absorbance was monitored for approximately 5 min and irradiation was repeated if no significant absorbance decay was observed. This was the case for the first pulses, presumably because traces of oxygen and other impurities scavenged the reactive radicals. After a few pulses the absorbance started to decrease, and this process was recorded as a function of time. These UV/vis experiments were repeated two or three times for separately prepared **1a**/PR_3 (1:50) solutions having the same composition, and the results appeared to be reproducible within 10%.

Electrochemistry. Cyclic voltammetric measurements were performed with a PAR Model 173 potentiostat equipped with a PAR Model 176 I/E converter and connected to a PAR Model 175 universal programmer. Differential pulse voltammetric measurements were performed with a PAR polarographic analyzer (Model 174 A). IR and UV/vis spectra were measured on a Perkin-Elmer 1720-X FTIR and a Perkin-Elmer Lambda 9 UV/vis spectrometer, respectively. A three-electrode system was used which consisted of a platinum-disk working electrode, a platinum-plate auxiliary electrode, and a Ag/Ag^+ (0.1 M AgOTf) reference electrode in THF. The last electrode was separated from the sample solution by a glass frit. The sample solution contained the supporting electrolyte (0.1 M TBAH) and an approximately 10^{-3} M solution of the compound under study. Cyclic voltammograms were recorded at a scan rate of 100 mV s^{-1} unless stated otherwise and differential pulse voltammograms at a scan rate of 5 mV s^{-1} with a pulse frequency of 2 Hz. Controlled-potential electrolyses were carried out with a Wenking LB 75 M potentiostat and a Birtley electronic integrator. A cyclic voltammogram of the sample in the electrolysis cell was recorded before starting the electrolysis; the electrolysis potential was carefully chosen so that other reductions, taking place at higher potentials, did not occur. All measurements were carried out on THF solutions; samples were prepared and measured in a nitrogen-containing glovebox. Solutions of the complexes were kept in the dark to avoid photochemical decomposition. The half-wave potential of the ferrocene/ferrocenium couple was measured for a 10^{-3} M ferrocene solution in THF at the start of each experimental session under exactly the same conditions ($E^0(Fc^+/Fc)$ = −0.22 V vs Ag/Ag^+). All potentials are given vs a saturated calomel electrode (SCE); the conversions were made by using the reported value of $E_{1/2}(Fc^+/Fc)$ in THF vs SCE.[17]

Preparative-Scale Electrochemical Reductions. $(CO)_5MnMn(CO)_3$(bpy′) (1a). **1a** (35 mg) was dissolved in 20 mL of THF. The electrolysis was performed at a potential of −1.39 V. The initial current was 4.7 mA. The electrolysis was stopped when the current diminished to 5% of the initial value, and this was accomplished with 6.5×10^{-5} C (0.9 faraday of charge/mol of **1a**). IR spectra taken of the electrolyzed solution showed that the IR ν(CO) bands belonging to the starting compound had disappeared while new ones were observed at 1897 (s) and 1864 (vs) cm^{-1} and at 1974 (m), 1930 (m), and 1879 (sh) cm^{-1} belonging to $Mn(CO)_5^-$[18] and **2a**, respectively. In addition, the intense MLCT band of **2a** appeared at 848 nm.[12] The reduction wave of the starting compound had disappeared in the cyclic voltammogram that was taken from the electrolyzed solution. A reduction peak at −1.65 V and oxidation peaks in the backward scan at −1.07 and −0.08 V were present instead.

$[Mn(CO)_3$(bpy′)$(P(nBu)_3)]^+$. $[Mn(CO)_3$(bpy′)$(P(nBu)_3)]$[OTf] (18 mg), 132 mg of **1a** and 320 μL of $P(nBu)_3$ (1:9.5:50) were

(11) Andréa, R. R.; de Lange, W. G. J.; van der Graaf, T.; Rijkhoff, M.; Stufkens, D. J.; Oskam, A. *Organometallics* **1988**, *7*, 1100.
(12) Kokkes, M. W.; de Lange, W. G. J.; Stufkens, D. J.; Oskam, A. *J. Organomet. Chem.* **1985**, *294*, 59.
(13) Stiegman, A. E.; Stieglitz, M.; Tyler, D. R. *J. Am. Chem. Soc.* **1983**, *105*, 6032.
(14) Bock, H.; tom Dieck, H. *Chem. Ber.* **1967**, *100*, 228.
(15) (a) Morse, D. L.; Wrighton, M. S. *J. Am. Chem. Soc.* **1976**, *98*, 3931. (b) Staal, L. H.; van Koten, G.; Vrieze, K. *J. Organomet. Chem.* **1979**, *175*, 73.
(16) Grant, S. M.; Manning, A. R. *Inorg. Chim. Acta* **1978**, *31*, 41.
(17) $E_{1/2}(Fc^+/Fc)$ = +0.530 ≙ 0.003 V vs SCE (0.1 M TBAP in THF).[8]
(18) York Darensbourg, M.; Darensbourg, D. J.; Burns, D.; Drew, D. A. *J. Am. Chem. Soc.* **1976**, *98*, 3127.

Table I.[a] Photochemical Reactions of 1/PR_3 Mixtures

	L, ν(CO),[b] θ[c]						
compd	NEt_3, 1915, 132[d]	py, 1917,[e]	$P(cHex)_3$, 1937, 170	$P(nBu)_3$, 1940, 132	PPh_3, 1950, 145	$P(OMe)_3$, 1964, 107	$P(OPh)_3$, 1970, 128
1a	ET/D	ET	ET	ET	ET/D	ET/D	ET/D
1c				ET			
1b				ET			
1b'				ET			
1b''	ET/D			ET	D		

[a] Conditions and legend: molar ratio 1:L = 1:50 in THF at 298 K; λ_{irr} = 546 nm; ET = reaction 4; D = radical dimerization reactions; ET/D = both reactions observed. [b] Wavenumber of A_1 ν(CO) band of $Mo(CO)_5(L)$ from ref 13. [c] Cone angle θ in deg from ref 21. [d] θ from PEt_3. [e] Cone angle unspecified because of planar pyridine structure.

dissolved in 20 mL of THF. The sample was very light sensitive due to the photocatalytic activity of **1a**/$P(nBu)_3$ mixtures. Hence, the sample was prepared and kept in the dark; 5 mL of it was placed in a glass vessel next to the electrolysis cell as a blank solution, and the other 15 mL was used for the electrolysis experiment. The applied potential (−1.11 V) was switched off when 1.00×10^{-5} C (0.48 faradays of charge/mol of cation) had passed. IR spectra were taken from the electrolyzed and blank solutions to determine the conversion of **1a** and to ascertain that the reactions were not initiated photochemically. Approximately 45% of the initial amount of **1a** had reacted in the electrolysis cell, while less than 5% had reacted photochemically in the blank solution (conversion rates were calculated from the decrease of the 1981-cm^{-1} band of **1a**). This means that the conversion of **1a** in the electrolysis cell was initiated electrochemically. $Mn(CO)_5^-$ and $Mn(CO)_3(bpy')(P(nBu)_3)^+$ were identified by their CO stretching frequencies as the products in both solutions.

$[Mn(CO)_3(iPr\text{-}DAB)(PPh_3)]^+$ in the Presence of $Ru_3(CO)_{12}$. $[Mn(CO)_3(iPr\text{-}DAB)(PPh_3)][OTf]$, (24 mg), 200 mg of $Ru_3(CO)_{12}$, and 440 mg of PPh_3 (1:10:50) were dissolved in 20 mL of THF. The reduction was performed at −0.82 V and was stopped when 1.44×10^{-5} C (0.41 faradays of charge/mol of cation) had passed. New bands belonging to $Ru_3(CO)_{11}(PPh_3)$ (2097 (w), 2046 (m), 2015 (s) cm^{-1})[19] and $Ru_3(CO)_{10}(PPh_3)_2$ (2072 (w), 1995 (s br) cm^{-1})[19] were observed in the IR spectrum of the electrolyzed solution, while the CO stretching bands of $Ru_3(CO)_{12}$ had completely disappeared.

In a different experiment, it was ascertained whether the electrochemical measurements had been influenced by the thermal substitution of CO by PPh_3.[20] For this purpose, the thermal reaction of a $Ru_3(CO)_{12}/PPh_3$ (1:5) mixture in THF was followed with IR spectroscopy. Less than 5% of the $Ru_3(CO)_{12}$ (calculated from the decrease of the CO band at 2060 cm^{-1}) was converted after 1 h, the time needed for the electrolysis. This proves that the yield of the thermal CO substitution can be neglected during the electrolysis experiment and, consequently, that the $Ru_3(CO)_{12}$ conversion during the reduction of $Mn(CO)_3(iPr\text{-}DAB)(PPh_3)^+$ is a true electrochemical process.

Results

A. Electron-Transfer Reactions of Complexes 1 in the Presence of L. L = P-Donor Ligand. Irradiation of a solution of **1** and $P(nBu)_3$ (1:50) in THF gave rise to the photocatalytic production of $Mn(CO)_5^-$ and $Mn(CO)_3(\alpha\text{-diimine})(P(nBu)_3)^+$ according to reaction 4. The

$$1 + PR_3 \xrightarrow{h\nu} Mn(CO)_5^- + Mn(CO)_3(\alpha\text{-diimine})(PR_3)^+ \quad (4)$$

photoproducts were characterized by their CO stretching frequencies. The involvement of radical species in the reaction was evident from the observation that the reaction was completely quenched by addition of the radical scavenger CCl_4. Thus, irradiation of a solution of **1a**, $P(OMe)_3$, and CCl_4 (1:50:100) in THF only produced $Mn(CO)_5Cl$ and $Mn(CO)_3(bpy')Cl$. Reaction 4 was followed with IR spectroscopy for different mixtures of **1a** and PR_3 in order to establish the influence of the phosphine ligands on the efficiency of the reaction. This efficiency appeared to be lowest for bulky and for very weakly electron donating PR_3 ligands.[21] Irradiation of a solution containing such a ligand did not give rise to reaction 4 but instead produced **2a**, $Mn_2(CO)_{10}$ and $Mn_2(CO)_8(PR_3)_2$. This result demonstrates that radical coupling and substitution reactions prevail in these mixtures. The reactions taking place for various mixtures of complexes and ligands are summarized in Table I. ET and D denote that the electron transfer reaction (4) or the dimerization reactions predominate, respectively. ET/D refers to samples in which both reactions occur with a reasonable yield. In the UV/vis spectra, reaction 4 was accompanied by a rapid disappearance of the MLCT band of the starting complex, while a weak absorption band of the $Mn(CO)_3(\alpha\text{-diimine})(PR_3)^+$ cation showed up between 400 and 500 nm (see Figure 2).

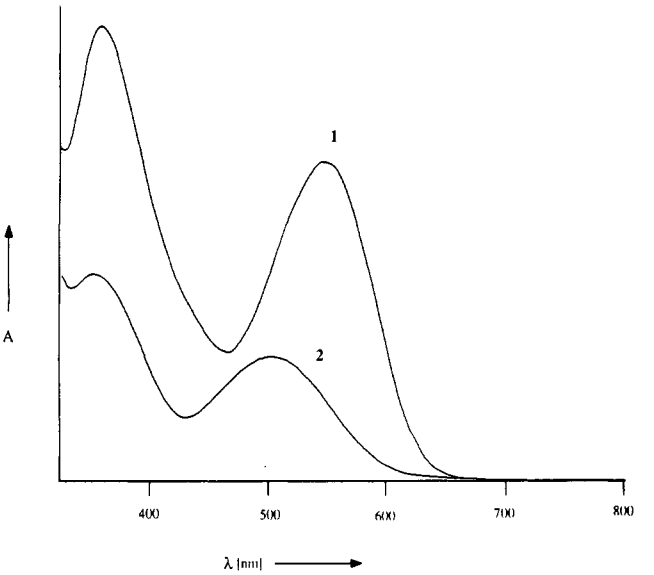

Figure 2. UV/vis absorption spectra of a **1a**/$P(nBu)_3$ (1:200) mixture in toluene before (1) and after (2) irradiation with 514.5-nm light.

The catalytic nature of reaction 4 was evident from the extreme light sensitivity of the $1/PR_3$ solutions and from the observation that the reaction proceeded in the dark after a few light pulses. No appreciable thermal conversion was observed when these solutions were not irradiated but kept in the dark for the same period of time. In order to study the influence of the PR_3 ligand on the rate of reaction 4, the UV/vis spectral changes taking place after

(19) Bruce, M. I.; Matisons, J. G.; Nicholson, B. K. *J. Organomet. Chem.* **1983**, *247*, 321.
(20) Candlin, J. P.; Shortland, A. C. *J. Organomet. Chem.* **1969**, *16*, 289.
(21) For steric and electronic parameters see: Tolman, C. A. *Chem. Rev.* **1977**, *77*, 313.

a few light pulses were recorded for different **1a**/PR_3 (1:50) solutions as described in the Experimental Section. The reproducibility of these experiments was carefully checked by repeating them two or three times for solutions having the same composition.

The cone angle dependence was established for the phosphines $P(nBu)_3$, $P(iBu)_3$, and $P(cHex)_3$, having strongly differing cone angles but similar basicities.[21] Photodisproportionation was then only observed for solutions containing $P(nBu)_3$. Solutions containing the bulkier ligands $P(iBu)_3$ and $P(cHex)_3$ only showed dimerization of the photoproduced radicals. The influence of the basicity was studied by comparing the behavior of the phosphines $P(nBu)_3$, $P(MePh_2)$, $P(OiPr)_3$, and $P(OPh)_3$, which have different basicities but almost the same cone angle. The rate of reaction 4 then decreased in the above order, and in the case of $P(OPh)_3$ hardly any photodisproportionation was observed. Rate constants could not be determined since the concentration of the radicals was not known. Values in which this concentration is incorporated are also not meaningful since the radical concentration strongly depends on the specific experimental conditions of these measurements.

L = O- or N-Donor Ligand. Irradiation at room temperature of the complexes **1** in neat THF did not lead to photodisproportionation but instead gave rise to the radical coupling reactions. Photodisproportionation into $Mn(CO)_5^-$ and $Mn(CO)_3(\alpha\text{-diimine})(S)^+$ (S = THF, 2-MeTHF) only occurred at $T < 200$ K. When the temperature of the product solution was raised, the ions reacted back with each other to give the parent complex. The same reaction was observed when solutions of $Mn(CO)_5^-$ and $Mn(CO)_3(bpy')(THF)^+$ were mixed at room temperature. Obviously, the driving force for the photodisproportionation reaction is supplied by a reaction of the $Mn(CO)_3(\alpha\text{-diimine})S^\bullet$ radical adducts. Only if the sample solution contains an appreciable amount of these adducts does electron transfer to the parent complex take place. Otherwise, the $Mn(CO)_3(\alpha\text{-diimine})^\bullet$ radicals undergo radical coupling reactions.

Similar behavior was observed upon irradiation of these complexes in the presence of a N-donor ligand. Irradiation at room temperature of a 1/N-donor (1:50; N-donor = pyridine, NEt_3) mixture dissolved in THF gave rise to the formation of both radical coupling and disproportionation products. The relative yield of the disproportionation products increased when a larger excess of the N-donor ligand was used. Thus, the radical coupling reaction was completely suppressed when **1a** was irradiated in neat pyridine (molar ratio 1:10[5]).

The different coordinating abilities of the nitrogen- and phosphorus-donor ligands with respect to the $Mn(CO)_3(\alpha\text{-diimine})^\bullet$ radicals also became apparent when a mixture of **1a**, pyridine, and $P(OMe)_3$ (1:50:50), dissolved in THF, was irradiated. Only the cation $Mn(CO)_3(bpy')(P(OMe)_3)^+$ was then formed in addition to $Mn(CO)_5^-$. This demonstrates that $Mn(CO)_3(bpy')^\bullet$ radicals preferably form adducts with phosphine ligands.

Reduction Potentials of Complexes 1 and $Mn(CO)_3(\alpha\text{-diimine})(PR_3)^+$. Complexes 1. Just as for $Cp_2Mo_2(CO)_6$, $Cp_2Fe_2(CO)_4$, and $Mn_2(CO)_{10}$, the key step of the photodisproportionation reaction (4) of these complexes is proposed to be the transfer of an electron to the parent compound. Because of this, the electrochemistry of these complexes has been studied with cyclic voltammetry (CV) and differential pulse voltammetry (DPV). The compounds exhibited a complex electrochemical behavior, and many irreversible[51] oxidation and reduction waves were observed in the cyclic voltammograms. Cyclic voltammograms of complex **1c** are shown as typical examples in parts a and b of Figure 3 (recorded between −2.3 and +0.6 V and between −1.4 and +0.6 V, respectively). They show the presence of two irreversible reduction waves I and II at −1.22 and −1.44 V. DPV was employed to obtain better resolved waves.

Table II.[a] Cathodic Peak Potentials E_{pc} and E_p of Manganese Compounds

$Mn_2(CO)_{10}$

compd	E_{pc}[b]	E_p[c]
$Mn_2(CO)_{10}$	−1.42	−1.29
	−1.88	

$(CO)_5MM'(CO)_3(\alpha\text{-diimine})$

M	M'	α-diimine	compd	E_{pc}[b]	E_p[c]
Mn	Mn	pAn-DAB	**1b'**	−0.84	−0.78
				−1.28	−1.23
Mn	Mn	pAn-DAB(Me,Me)	**1b''**	−1.04	−0.98
				−1.29	−1.23
Mn	Mn	iPr-DAB	**1b**	−1.18	−1.08
				−1.26	−1.19
Mn	Mn	iPr-PyCa	**1c**	−1.22	−1.14
				−1.44	−1.44
Mn	Mn	bpy'	**1a**	−1.35	−1.26
				−1.59	−1.59

$[Mn(CO)_3(\alpha\text{-diimine})(PR_3)][OTf]$

α-diimine	PR_3	ν(CO)[d]	E_{pc}[b]	E_p[c]
iPr-DAB	$P(OPh)_3$	2085.3	−0.69	−0.65
			−0.88	−0.84
			−1.25	−1.18
iPr-DAB	$P(OMe)_3$	2079.5	−0.74	−0.69
			−0.83	−0.78
			−1.07	−1.03
			−1.22	−1.16
iPr-DAB	PPh_3	2068.9	−0.71	−0.71
			−0.89	−0.84
			−1.16	−1.08
			−1.29	−1.23
iPr-DAB	PMe_2Ph	2065.3	−0.88	−0.86
			−1.05	−1.02
iPr-DAB	$P(nBu)_3$	2060.3	−0.89	−0.83
			−1.23	−1.19
iPr-PyCa	$P(nBu)_3$	2060.3	−1.06	−1.00
			−1.22	−1.18
			−1.42	−1.39
bpy'	$P(nBu)_3$	2060.3	−1.22	−1.17
			−1.40	−1.36
			−1.62	−1.55

[a] Potentials in V vs SCE, measured in THF containing 0.1 M TBAH. [b] Cathodic peak potentials from CV recorded at a scan rate of 100 mV s^{-1}. [c] Peak potentials from DPV, recorded at a scan rate of 5 mV s^{-1}. [d] Wavenumber of A_1 ν(CO) band of $Ni(CO)_3(PR_3)$ from ref 21.

The reduction potentials of several $(CO)_5MnMn(CO)_3(\alpha\text{-diimine})$ compounds are listed in Table II. The peak potentials of CV and DPV measurements, E_{pc} and E_p, respectively, differ by 50–100 mV as can be expected for completely irreversible electron-transfer reactions. The peak potential of the first reduction wave, $E_{pc}(I)$, varies with the α-diimine ligand and decreases from −0.84 to −1.35 V upon going from the R-DAB to the bpy' complex.

One of the objectives was to clarify the mechanism of the reduction of complex **1**. Spectroscopic analysis following the preparative-scale reduction of **1a** (see Experimental Section) showed that Mn–Mn bond fission took place by the uptake of one electron. The metal–metal-bonded complex anion then decomposed, producing $Mn(CO)_5^-$ and $Mn(CO)_3(bpy')^\bullet$ radicals, which dimerized to give **2a**. The complete irreversibility of reduction wave I in Figure 3 shows that the decomposition of **1** proceeds

Scheme I

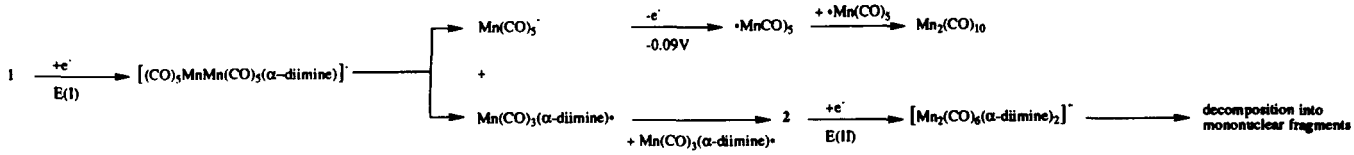

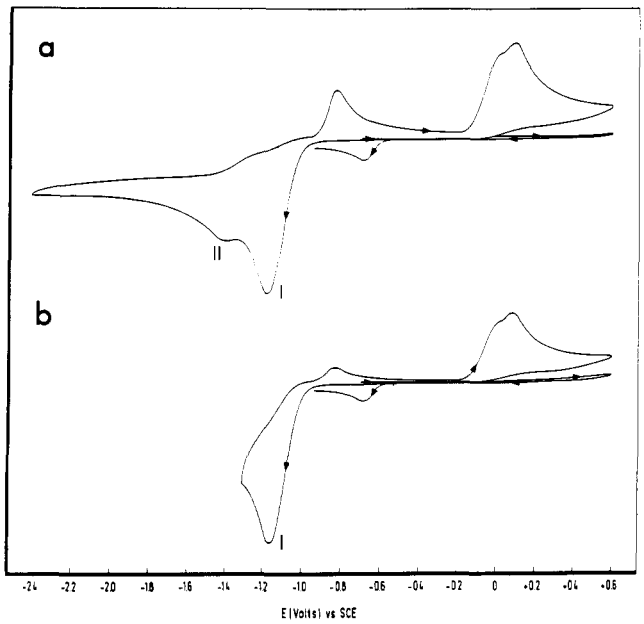

Figure 3. *Cyclic voltammograms of* **1c** *in THF containing* 0.1 M TBAH, recorded at a scan rate of 100 mV s^{-1} and starting from −0.7 V in the positive direction between (a) −2.4 and +0.6 V and (b) −1.3 and +0.6 V.

rapidly.[22,23] The redox waves of the two electrolysis products $Mn(CO)_5^-$ and **2** were identified. An oxidation wave with $E_{p,a}$ = −0.09 V, which is also present in the CV of $Mn_2(CO)_{10}$, was previously assigned to the oxidation of $Mn(CO)_5^-$.[24] Waves belonging to **2** were determined by recording the cyclic voltammogram of **2c**. Only one reduction wave at −1.41 V was detected in the cyclic voltammogram scanned between −1.6 and +0.6 V. The peak potential corresponded to that of wave II in the cyclic voltammogram of **1c** in Figure 3a (E_{pc}(II) = −1.44 V). These waves are therefore assigned to the reduction of **2**. The spectroscopic and voltammetric results of the reduction of **1** are in accordance with each other; the reduction and subsequent reactions are summarized in Scheme I.

$Mn(CO)_3(\alpha$-diimine$)(PR_3)^+$. Cyclic voltammograms of $Mn(CO)_3(\alpha$-diimine$)(PR_3)^+$ cations were recorded to determine the potential at which the $Mn(CO)_3(\alpha$-diimine$)(PR_3)^•$ radicals are oxidized. These species are thought to be the key intermediates in the photodisproportionation (eq 4). Unfortunately, these attempts were not successful since the radicals, formed in the forward scan by the reduction of $Mn(CO)_3(\alpha$-diimine$)(PR_3)^+$, were too short-lived to perceive their oxidation wave in the backward scan. Typical examples of the $Mn(CO)_3(\alpha$-diimine$)(PR_3)^+$ cyclic voltammograms are given in Figure

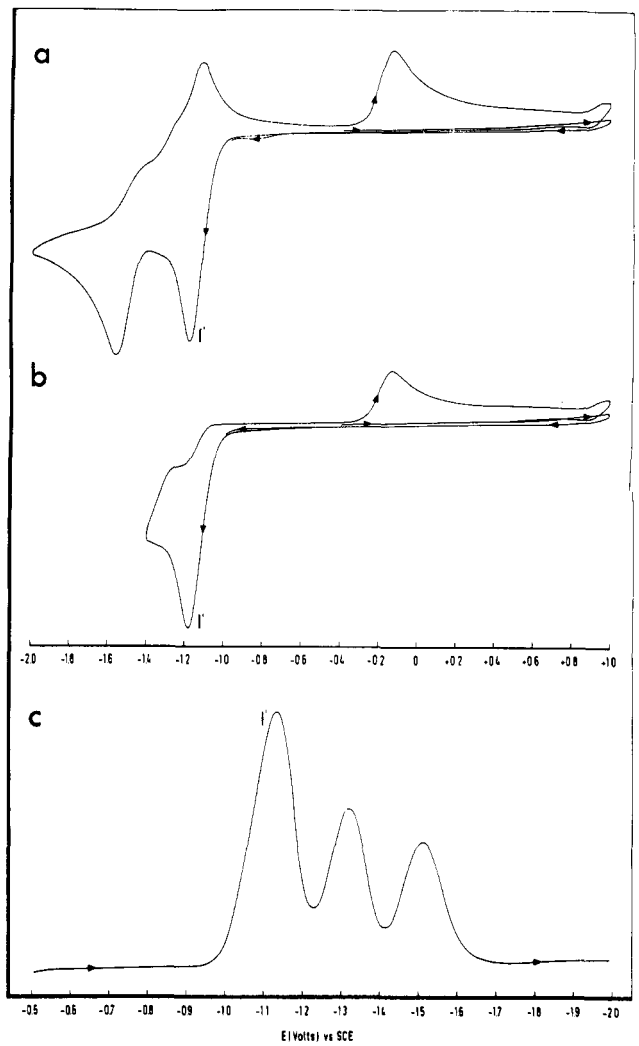

Figure 4. Cyclic voltammograms of $[Mn(CO)_3(bpy')(P(nBu)_3)][OTf]$ in THF containing 0.1 M TBAH, recorded at a scan rate of 100 mV s^{-1} and starting from −0.4 V in the positive direction between (a) −2.0 and +1.0 V and (b) −1.3 and +1.0 V. (c) Differential pulse voltammogram of the same solution recorded at a scan rate of 5 mV s^{-1} between −0.5 and −2.0 V.

4a,b, which shows the traces for $Mn(CO)_3(bpy')(P(nBu)_3)^+$ scanned between −2.0 and +1.0 V (Figure 4a) and between −1.3 and +1.0 V (Figure 4b). The cyclic voltammograms display the irreversible reduction wave I′ that remains totally irreversible when the scan rate is increased from 100 mV s^{-1} to 100 V s^{-1}. I′ is overlapped by another wave at a slightly lower potential. The better resolving properties of DPV needed for an accurate determination of E_p(I′) is illustrated by Figure 4c. The peak potentials of I′ and other nearby waves are listed in Table II. The widths of the DPV and CV waves I′ at half-height vary between 130 and 190 mV. These numbers, well above the limiting value of 90.4 mV for reversible one-electron reductions, agree with the irreversibility of I′.[25]

(22) The other $(CO)_5MM'(CO)_3(bpy')$ (M, M′ = Mn, Re) dimers were analyzed as well. Nevertheless, even for M = Re, M′ = Mn, i.e. the dimer with the strongest M–M′ bond,[23] completely irreversible reduction waves were recorded at scan rates as high as 100 V s^{-1}.

(23) Meckstroth, W. K.; Ridge, D. P. *J. Am. Chem. Soc.* **1985**, *107*, 2281.

(24) (a) Lacombe, D. A.; Anderson, J. E.; Kadish, K. M. *Inorg. Chem.* **1986**, *25*, 2074. (b) Lee, K. Y.; Kuchynka, D. J.; Kochi, J. K. *Organometallics* **1987**, *6*, 1886.

(25) Bard, A. J.; Faulkner, L. R. *Electrochemical Methods*; Wiley: New York, 1980.

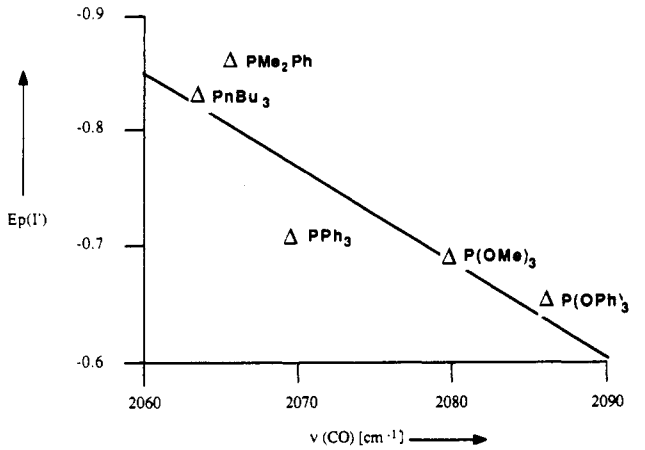

Figure 5. E_p values of $Mn(CO)_3(iPr\text{-}DAB)(PR_3)^+$ vs the A_1 $\nu(CO)$ wavenumber of $Ni(CO)_3(PR_3)$.

The influence of the α-diimine ligand on the $Mn(CO)_3(\alpha\text{-diimine})(PR_3)^+$ reduction potential was established in the reduction of a series of $Mn(CO)_3(\alpha\text{-diimine})(P(nBu)_3)^+$ ions. Just as for the complexes **1**, $E_p(I')$ decreases upon going from the iPr-DAB to the bpy′ cations. In addition, cyclic voltammograms of several $Mn(CO)_3(iPrDAB)(PR_3)^+$ ions were recorded in order to measure the dependence of $E_p(I')$ on PR_3. Values of $E_p(I')$ and $E_{pc}(I')$ are listed in Table II, and $E_p(I')$ is depicted as a function of the phosphine basicity in Figure 5. $E_p(I')$ shifts to more negative potentials for more basic phosphines, a trend which has been observed before for many other phosphine-substituted compounds.[26]

Although no oxidation potentials of $Mn(CO)_3(\alpha\text{-diimine})(PR_3)^\bullet$ radicals could be determined from the cyclic voltammograms of $Mn(CO)_3(\alpha\text{-diimine})(PR_3)^+$, their reducing power could still be established in a preparative-scale reduction. $[Mn(CO)_3(bpy')(P(nBu)_3)]^+$ was reduced in the presence of **1a** and $P(nBu)_3$ (1:9.5:50), and 45% of **1a** was converted when 0.48 faraday of charge/mol of $[Mn(CO)_3(bpy')(P(nBu)_3)][OTf]$ had passed through the solution (see Experimental Section). This means that the $Mn(CO)_3(bpy')(P(nBu)_3)^\bullet$ radical, formed by the reduction of $Mn(CO)_3(bpy')(P(nBu)_3)^+$, catalyzes the disproportionation of **1a** in the presence of phosphines with a turnover number of at least 9.

B. Electron-Transfer Reactions of 1 in the Presence of PR_3 and $M_3(CO)_{12-x}(PR_3)_x$ (M = Fe, Ru, Os; x = 0–2) Clusters. The reactions between $Mn(CO)_3(\alpha\text{-diimine})(PR_3)^\bullet$ radicals and electron acceptors A having various reduction potentials were studied in order to determine the reducing strength of the radicals. For this purpose, solutions of $1/PR_3/A$ (1:50:1) were irradiated and the reactions taking place were compared with those of mixtures of A and PR_3 (1:50). A different conversion rate of A in the two samples then showed that the manganese radicals had reacted with A. Several $M_3(CO)_{12-x}(PR_3)_x$ (M = Fe, Ru, Os; x = 0–2) clusters were used as electron acceptor A. These clusters were chosen since they may undergo an electron transfer chain (ETC) reaction in which a CO ligand is substituted (reaction 5).[3k,27]

$$M_3(CO)_{12-x}(PR_3)_x + PR_3 \xrightarrow{[+e^-]} M_3(CO)_{11-x}(PR_3)_{x+1} + CO \quad (5)$$

M = Fe, Ru, Os

(26) For examples of this see: (a) Kuchynka, D. J.; Amatore, C.; Kochi, J. K. *Inorg. Chem.* **1986**, *25*, 4087. (b) Hershberger, J. W.; Kochi, J. K. *Polyhedron* **1983**, *2*, 929.

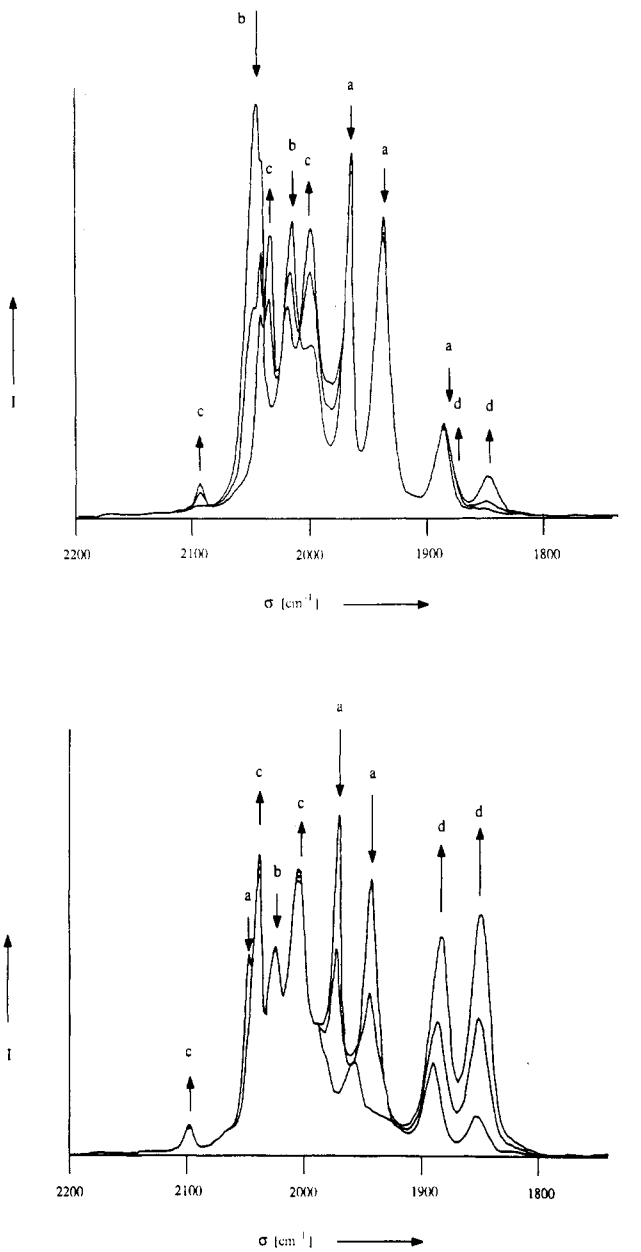

Figure 6. IR spectral changes for a THF solution of a **1a**/$P(OMe)_3/Ru_3(CO)_{12}$ (1:50:10) mixture during irradiation with 546-nm light: (top) the initial photoreaction; (bottom) the subsequent photoreaction. CO bands are labeled as follows: (a) **1a**; (b) $Ru_3(CO)_{12}$; (c) $Ru_3(CO)_{11}P(OMe_3)$; (d) $Mn(CO)_5^-$.

Addition of 1 to the A/PR_3 mixture did not accelerate reaction 5 in the case of $Os_3(CO)_{12}$. It catalyzed, however, the substitution reactions of some iron and ruthenium clusters. The reactions of $1/PR_3/A$ mixtures are summarized in Table III. Cyclic voltammograms were recorded of the $M_3(CO)_{12-x}(PR_3)_x$ (M = Fe, Ru, Os; x = 0–2) compounds in order to determine their reduction potentials. With the exception of $Fe_3(CO)_{12}$ all clusters showed irreversible reductions and peak potentials varied between −0.39 and −1.71 V (Table III). A full description of the $M_3(CO)_{12-x}(PR_3)_x$ electrochemistry has been given before.[28]

Irradiation of a THF solution of **1a**, $P(OMe)_3$, and $Ru_3(CO)_{12}$ (1:50:10) gave rise to the catalytic substitution

(27) (a) Miholová, D.; Vlcek, A. A. *J. Organomet. Chem.* **1985**, *279*, 317. (b) Bruce, M. I.; Kehoe, D. C.; Matisons, J. G.; Nicholson, B. K.; Rieger, P. H.; Williams, M. L. *J. Chem. Soc., Chem. Commun.* **1982**, 442.

(28) (a) Bond, A. M.; Dawson, P. A.; Peake, B. M.; Robinson, B. H.; Simpson, J. *Inorg. Chem.* **1977**, *16*, 2199. (b) Cyr, J. C.; DeGray, J. A.; Gosser, D. K.; Lee, E. S.; Rieger, P. H. *Organometallics* **1985**, *4*, 950.

Table III. Photochemical Reactions of 1a/P(OMe)$_3$/A Mixtures and Cathodic Peak Potentials E_{pc} of A (A = $M_3(CO)_{12-x}(PR_3)_x$ (M = Fe, Ru, Os))

$M_3(CO)_{12-x}(PR_3)_x$	photoreaction[a]	E_{pc}[b]
$Fe_3(CO)_{12}$	(6)	−0.39
$Fe_3(CO)_{10}(P(OPh)_3)_2$	(6)	−1.00
$Ru_3(CO)_{12}$	(6)	−1.05
$Fe_3(CO)_{10}(P(OMe)_3)_2$	(6)	−1.09
$Fe_3(CO)_9(P(OPh)_3)_3$	(3)	−1.32
$Os_3(CO)_{12}$	(3)	−1.38
$Ru_3(CO)_{11}P(OPh)_3$	(3)	−1.71

[a] Conditions: molar ratio 1a:P(OMe)$_3$:A = 1:50:1 in THF at 293 K; λ_{irr} = 546 nm. [b] Cathodic peak potentials in V vs SCE, from CV, recorded in THF containing 0.1 M TBAH at a scan rate of 100 mV s^{-1}.

of CO in $Ru_3(CO)_{12}$ by P(OMe)$_3$ according to reaction 6 (Figure 6, top). When all the $Ru_3(CO)_{12}$ had reacted,

$$M_3(CO)_{12} + PR_3 \xrightarrow[1]{h\nu} M_3(CO)_{11}(PR_3) + CO \qquad (6)$$

complex 1a started to disproportionate according to reaction 4 (Figure 6, bottom). Since the $M_3(CO)_{12}$ clusters are known to react both thermally and photochemically with phosphines,[3a,20,29] the photochemistry of the $M_3(CO)_{12}/PR_3$ mixtures was also studied in the absence of complex 1a. THF solutions of $M_3(CO)_{12}/PR_3$ (1:50) were irradiated for $^1/_2$ h, during which time the $M_3(CO)_{12}$ conversion was monitored by the decrease of its intense carbonyl band at 2060 cm^{-1} (M = Ru) and 2049 cm^{-1} (M = Fe), respectively. The rate of reaction 6 was greater for more basic phosphines, but for all phosphines (except for P(nBu)$_3$) it was more than 2 orders smaller than that of the solutions to which 1 equiv of complex 1 was added. Reaction 6 was the only reaction observed for the $Ru_3(CO)_{12}$ cluster; a more complicated reaction was found for $Fe_3(CO)_{12}$, since the $Fe_3(CO)_{11}(PR_3)$ product decomposed into the $Fe(CO)_4(PR_3)$ and $Fe(CO)_3(PR_3)_2$ monomers. The fragmentation of $Fe_3(CO)_{11}(PR_3)$ also occurred during the photolysis of the $1/PR_3/Fe_3(CO)_{12}$ mixtures. Because of this, the course of reaction 6 was followed by the disappearance of $M_3(CO)_{12}$ instead of by the formation of $M_3(CO)_{11}(PR_3)$. The mechanism of the catalytic substitution was studied by varying systematically the composition of the $1/PR_3/M_3(CO)_{12}$ mixtures.

First of all, both reactions 4 and 6 were suppressed by the addition of a 50-fold excess of CCl_4 to a THF solution of 1a/P(OMe)$_3$/$Ru_3(CO)_{12}$ (1:50:1). Irradiation of this mixture only afforded $Mn(CO)_5Cl$ and $Mn(CO)_3(bpy')Cl$. The quenching of reaction 6 proves that the active catalyst is produced out of the manganese radicals formed in the homolysis reaction (1).

The dependence of reaction 6 on the α-diimine was investigated by irradiating different $1/P(OMe)_3/M_3(CO)_{12}$ (M = Fe, Ru; 1:50:1) mixtures. The influence of the phosphine ligand on reaction 6 was investigated by comparing the yields of different $1a/PR_3/Ru_3(CO)_{12}$ (R = OPh, OMe, Ph, cHex; 1:50:1) mixtures. Unlike the example given in Figure 6, reactions 4 and 6 occurred simultaneously in most of these mixtures and the extent to which complex 1 reacted during the $M_3(CO)_{12}$ conversion depended on the α-diimine, PR_3 and M.

As mentioned above, the course of reaction 6 after the mixture was irradiated for a certain period was followed by recording the IR spectrum and by measuring the decrease of the most intense CO band of $M_3(CO)_{12}$. The calculated ratios $I_{2060,t}(Ru_3(CO)_{12})/I_{2060,t=0}(Ru_3(CO)_{12})$ and $I_{2049,t}(Fe_3(CO)_{12})/I_{2049,t=0}(Fe_3(CO)_{12})$ are denoted as $x_{(6)}$ in Table IV. The course of reaction 4 was followed from the same IR spectrum by measuring the decay of the intense carbonyl band of 1 near 1990 cm^{-1}. The resulting decay ratios $I_{1990,t}(1)/I_{1990,t=0}(1)$ are denoted as $x_{(4)}$ in Table IV. Table IV also presents the relative yields of reactions 6 and 4, $x_{(6)}/x_{(4)}$.

Table IV. Yields of Reactions 4 and 6, $x_{(4)}$ and $x_{(6)}$, in $1/L/M_3(CO)_{12}$ Mixtures

(a) α-Diimine Compounds (L = P(OMe)$_3$)

	M = Ru			M = Fe		
complex[a]	$x_{(6)}$[b]	$x_{(4)}$[b]	$x_{(6)}/x_{(4)}$	$x_{(6)}$[b]	$x_{(4)}$[b]	$x_{(6)}/x_{(4)}$
1a	0.82	0.16	5.2	0.59	0.01	48.6
1c	0.59	0.46	1.3	0.42	0.03	16.5
1b	0.32	0.56	0.6	0.70	0.06	11.6
1b′	<0.21[c]	1.00	<0.2	0.76	0.24	3.2

(b) Complex 1a (Various L)

L[d]	ν(CO)[e]	θ[f]	$x_{(6)}$[b]	$x_{(4)}$[b]	$x_{(6)}/x_{(4)}$
P(cHex)$_3$	1937	170	0.59	0.03	20.4
PPh_3	1950	145	0.92	0.10	9.5
P(OMe)$_3$	1964	107	0.82	0.16	5.2
P(OPh)$_3$	1970	128	0.48	0.10	4.8
py	1917	g	0.20	0.53	0.4

[a] Conditions: molar ratio 1:P(OMe)$_3$:$M_3(CO)_{12}$ = 1:50:1 in THF at 293 K; λ_{irr} = 546 nm. [b] $x_{(6)}$ = yield of reaction 6; $x_{(4)}$ = yield of reaction 4 (see text). [c] Influenced by the decrease of overlapping $Ru_3(CO)_{12}$ bands. [d] Conditions: molar ratio 1a:L:$Ru_3(CO)_{12}$ = 1:50:1 in THF at 293 K; λ_{irr} = 546 nm. [e] Wavenumber of A_1 ν(CO) band of $Mo(CO)_5(L)$ from ref 13. [f] Cone angle θ in deg, from ref 21. [g] Unspecified because of planar pyridine structure.

Several trends emerge from these $x_{(6)}/x_{(4)}$ values. First, the extent to which $Ru_3(CO)_{12}$ was converted decreased upon going from the bpy′ to the iPr-DAB compound and the reaction was completely suppressed by the much faster disproportionation of complex 1 in the case of the pAn-DAB ligand. Second, for a given $1/PR_3$ combination the decrease of the $M_3(CO)_{12}$ concentration was always larger for M = Fe than for M = Ru. Finally, Table IVb shows that the basicity and not the cone angle of the phosphine determines the competition between reactions 6 and 4. A different dependence was found for the disproportionation reactions (4) of $1a/PR_3$ samples (vide supra), which appeared to be influenced by both the steric and electronic properties of the phosphines. On the other hand, reactions 4 and 6 in 1/L and $1/L/M_3(CO)_{12}$ mixtures respectively had lower yields for N- than for P-donor ligands L.

From the fact that reaction 6 is initiated by the radicals formed in reaction 1 and from the α-diimine and L dependence of $x_{(6)}/x_{(4)}$ it is concluded that the $Mn(CO)_3(\alpha\text{-diimine})(PR_3)^\bullet$ radical is not only responsible for the disproportionation of 1 but also initiates the cluster substitution (eq 6). This is supported by the reactions taking place upon reduction of $Mn(CO)_3(iPr\text{-}DAB)(PPh_3)^+$ in the presence of PPh_3 and $Ru_3(CO)_{12}$ (molar ratio 1:50:10) (see the Experimental Section). All the $Ru_3(CO)_{12}$ was then converted when 0.41 faraday of charge/mol of [$Mn(CO)_3$(iPr-DAB)(PPh_3)][OTf] had passed through the solution. This shows that the electrocatalytic substitution of $Ru_3(CO)_{12}$ has a turnover number of at least 24 and is initiated by the formation of $Mn(CO)_3(iPr\text{-}DAB)(PPh_3)^\bullet$ radicals.

Discussion

Mechanism of the Photochemical Disproportionation of 1. In the presence of certain phosphine ligands the disproportionation of complexes 1 is a very rapid catalytic reaction that starts upon irradiation into the

(29) (a) Shojaie, A.; Atwood, J. D. *Organometallics* **1985**, *4*, 187. (b) Desrosiers, M. F.; Wink, D. A.; Trautman, R.; Friedman, A. E.; Ford, P. C. *J. Am. Chem. Soc.* **1986**, *108*, 1917.

Scheme II

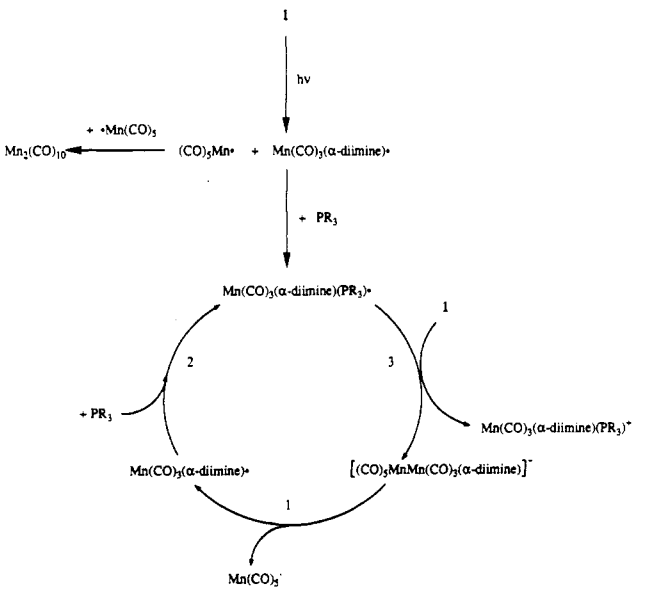

visible absorption band of the complex. As a result of this photoexcitation the complex undergoes homolysis of the Mn–Mn bond as well as release of CO.[30,31] It has been shown, however, that the CO-loss reaction does not contribute to the photodisproportionation reaction (4).[32] The reactions of the $•Mn(CO)_5$ and $Mn(CO)_3(\alpha\text{-diimine})•$ radicals formed in the homolysis reactions have been studied before.[33] The radicals themselves do not initiate the disproportionation, since the reaction only proceeds in the presence of the two-electron donor L. Nevertheless, the quenching of the disproportionation by addition of the radical scavenger CCl_4 to the 1/L mixture demonstrates that the reaction starts by homolysis of the Mn–Mn bond. In a previous ESR study it has been established that $M(CO)_3(\alpha\text{-diimine})(L)•$ radicals are 18e species having their unpaired electron in an unfavorable $\pi^*(\alpha\text{-diimine})$ orbital.[11] Such radicals, having their unpaired electrons in antibonding MO's, are known to be strong reducers and to catalyze many organic and organometallic reactions.[3d-g,4e] It was therefore suggested that the $Mn(CO)_3(\alpha\text{-diimine})(L)•$ radicals are responsible for the electron-transfer step in the disproportionation reaction (4).[12] The reducing power will then be strongest for the bpy′ radicals, since the π^* orbital of this ligand is higher in energy than those of the R-DAB and R-PyCa radicals.[34]

The electrochemical results are in agreement with this prediction and identified the subsequent steps of the catalytic cycle (see Scheme II). First, the cyclic voltammograms and the preparative-scale reduction of 1 showed that $[(CO)_5MnMn(CO)_3(\alpha\text{-diimine})]^-$ is an unstable anion that rapidly decomposes into $Mn(CO)_5^-$ and the $Mn(CO)_3(\alpha\text{-diimine})•$ radical (step 1 of the catalytic cycle in Scheme II). Second, the preparative-scale reduction of $Mn(CO)_3(bpy')(P(nBu)_3)^+$ in the presence of **1a** and $P(nBu)_3$ proved that $Mn(CO)_3(\alpha\text{-diimine})(PR_3)•$ radicals cause the disproportionation of 1. $Mn(CO)_3(\alpha\text{-diimine})(PR_3)•$ radicals thus transfer an electron to 1 (step 3), which subsequently decomposes (step 1). The catalytic cycle is closed by the associative reaction between the $M(CO)_3(\alpha\text{-diimine})•$ radical and the phosphine (step 2).[11]

The mechanism of the catalytic process displayed in Scheme II is similar to those of the $Cp_2Mo_2(CO)_6$, $Cp_2Fe_2(CO)_4$, $W_2(CO)_{10}^{2-}$, and $Mn_2(CO)_{10}$ disproportionations, in which $CpMo(CO)_3(PR_3)•$,[13] $CpFe(CO)_2(PR_3)•$,[35] $W(CO)_5(L)•^-$,[36] and $Mn(CO)_3(N)_3•$[37] radicals transfer an electron to the parent compound. The electronic structures of these species differ from those of the radicals under study, since they are 19-electron adducts having the unpaired electron in a more unfavorable metal-centered orbital. Because of this, such radicals are better reducing agents. Their electron-transfer reactions, including the catalyzed substitution of CO in $Ru_3(CO)_{12}$ by PR_3, have been reported and described in several review articles by Tyler et al.[3d,g,k,4d,f] Although their reducing strengths are smaller, the 18-electron radicals under study have the advantage that they can easily be prepared in high yield by irradiating complexes such as 1 with visible light. Before discussing the reactions of the $Mn(CO)_3(\alpha\text{-diimine})(PR_3)•$ radicals, we focus first on the mechanism of step I of Scheme II.

Mechanism of the Electrochemical Disproportionation of 1. The reaction pathway of the electrochemical reduction of 1, which is deduced from the spectroscopic and electrochemical data, is depicted in Scheme I. Scheme I is also of importance in the reduction of other metal–metal-bonded complexes such as $Mn_2(CO)_{10}$ and $Cp_2Mo_2(CO)_6$, two reactions that were recently studied.[24a,38] These studies, using the analytical criteria formulated by Nicholson and Shain,[39] pointed out that the dimer reductions follow an E_1CE_2 mechanism (eq 7): a reduction (E_1) followed by the decomposition (C) of the reduced compound into an anion and a radical that in turn is reduced in reduction E_2. A second, highly unlikely, E_1E_2C mechanism (eq 8) could, however, not completely be disregarded since the reduced parent compound was too unstable to be detected.

$$M_2(CO)_{2n} \xrightarrow{E_1} [M_2(CO)_{2n}]^- \xrightarrow{C} [M(CO)_n]^- + •M(CO)_n \xrightarrow{E_2} 2[M(CO)_n]^- \quad (7)$$

$$M_2(CO)_{2n} \xrightarrow{E_1} [M_2(CO)_{2n}]^- \xrightarrow{E_2} [M_2(CO)_{2n}]^{2-} \xrightarrow{C} 2[M(CO)_n]^- \quad (8)$$

In the case of the complexes 1, the E_1E_2C and E_1CE_2 mechanisms can be distinguished since the reductions E_1 and E_2 take place at different potentials. With coulometry it was established that the reduction of 1 is a one-electron process. The products of this reaction, $Mn(CO)_5^-$ and **2**, were easily identified spectroscopically. These findings prove unequivocally that the metal–metal bond is broken

(30) Andréa, R. R.; de Lange, W. G. J.; Stufkens, D. J.; Oskam A. *Inorg. Chem.* **1989**, *28*, 318.
(31) van der Graaf, T.; van Rooy, A.; Stufkens, D. J.; Oskam, A. Submitted for publication.
(32) The complexes under study were irradiated in toluene and 2-MeTHF at temperatures below 190 K in the presence of a phosphine ligand in order to exclude the possibility that the CO-loss reaction contributes to the catalytic disproportionation. Under these reaction conditions the CO-loss products $(CO)_4Mn(\mu\text{-}CO)Mn(CO)_2(\alpha\text{-diimine})$ were formed as the only stable photoproducts. Raising the temperature caused their thermal decomposition into $Mn(CO)_5^-$ and $Mn(CO)_2(\alpha\text{-diimine})(PR_3)_2^+$.[33] The IR bands of this cation were not observed upon irradiation of the $1/PR_3$ mixtures at room temperature, and this proves that the disproportionation was not triggered by the loss of CO.
(33) van der Graaf, T.; Stufkens, D. J.; Oskam, A.; Goubitz, K. *Inorg. Chem.* **1991**, *30*, 599.
(34) Reinhold, J.; Benedix, R.; Birner, P.; Hennig, H. *Inorg. Chim. Acta* **1979**, *33*, 209.
(35) Castellani, M. P.; Tyler, D. R. *Organometallics* **1989**, *8*, 2113.
(36) Silavwe, N. D.; Goldman, A. S.; Ritter, R.; Tyler, D. R. *Inorg. Chem.* **1989**, *28*, 1231.
(37) (a) Stiegman, A. E.; Tyler, D. R. *Inorg. Chem.* **1984**, *23*, 527. (b) Stiegman, A. E.; Goldman, A. S.; Philbin, C. E.; Tyler, D. R. *Inorg. Chem.* **1986**, *25*, 2976.
(38) Kadish, K. M.; Lacombe, D. A.; Anderson, J. E. *Inorg. Chem.* **1986**, *25*, 2246.
(39) Nicholson, R. S.; Shain, I. *Anal. Chem.* **1964**, *36*, 706.

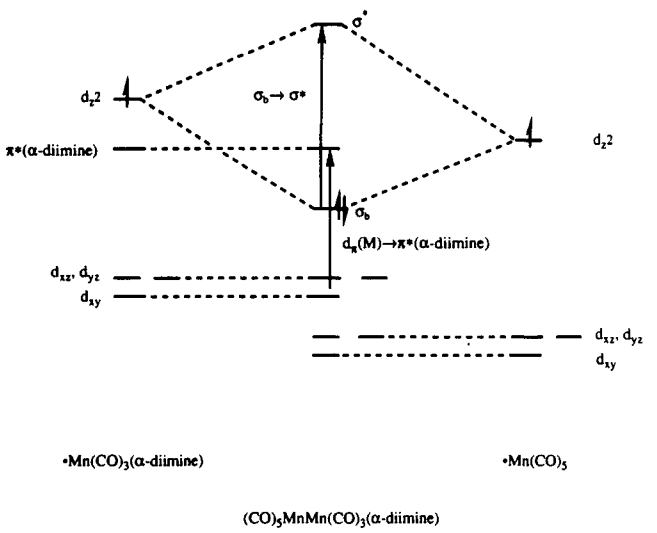

Figure 7. Qualitative molecular orbital diagram of 1.[10]

in an E_1C reaction and, consequently, that the overall reduction of these metal–metal-bonded dimers proceed along an E_1CE_2 mechanism.

In addition, the reduction potentials of 1 helped to identify which orbital is populated in the reduction E_1. According to the qualitative MO diagram (Figure 7)[15a,40] two molecular orbitals at relatively low energy were taken into account, viz. the metal–metal antibonding orbital (σ_{Mn-Mn}*) and an α-diimine-centered orbital (π*(α-diimine)). The reduction potentials E_{pc}(I) of 1 (Table II) are all higher than the E_{pc} value of $Mn_2(CO)_{10}$, and they shift to more negative values when the π*(α-diimine) orbital is raised in energy. For example, E_{pc} is higher for the iPr-DAB compound **1b** than for the bpy′ complex **1a**, and this is in accordance with the lower energy of the π* orbital of the iPr-DAB ligand compared to that of bpy′.[34] Likewise, E_{pc} of the iPr-DAB and iPr-PyCa compounds **1b,c** are almost the same (−1.18 and −1.22 V, respectively) since the π* orbitals of both α-diimine ligands are mainly localized at a C=N-iPr moiety. In addition, the reduction potential of the R-DAB compound is higher when R is an aromatic instead of an alkyl substituent and it decreases when the imine protons of the DAB ligand are replaced by the stronger σ-donating methyl group. A similar dependence of the reduction potential on the α-diimine ligand has been observed before for a series of Mo(CO)$_4$(α-diimine) complexes.[41] On the basis of these observations it is concluded that the π*(α-diimine) orbital and not the σ_{Mn-Mn}* orbital is occupied in the reduction of 1.

The thermal stability of such reduced α-diimine complexes varies from one complex to another. Thus, reduction of M(CO)$_4$(α-diimine) (M = Cr, Mo, W)[24a,b] or Ru(bpy)$_3^{2+}$[42] leads to the formation of radical complexes which are stable on the CV time scale (υ_{scan} = 100 mV s^{-1}). In the former case, however, the metal carbonyl fragment is already activated to some extent via spin delocalization from the nitrogen ligand to the cis carbonyls.[43] The reduced species of the corresponding BrRe(CO)$_3$(α-diimine) complexes decompose more easily by losing a Br$^-$ ligand.[44] The latter reaction is probably related to the decomposition of the reduced species [(CO)$_5$MnMn(CO)$_3$(α-diimine)]$^-$, according to reaction 9. The coordinatively

$$[(CO)_5MnMn(CO)_3(\alpha\text{-diimine})]^- \rightarrow Mn(CO)_5^- + Mn(CO)_3(\alpha\text{-diimine})^\bullet \quad (9)$$

unsaturated 16-electron radicals Mn(CO)$_3$(α-diimine)• formed by this reaction dimerize according to reaction 10.

$$2Mn(CO)_3(\alpha\text{-diimine})^\bullet \rightarrow \mathbf{2} \quad (10)$$

Reactions of Mn(CO)$_3$(α-diimine)(L)• Radicals. The reactions of **1a**/L mixtures (Table I) demonstrate that the yield of reaction 4 strongly depends on the properties of L. Variations in the disproportionation yield are caused by electronic and steric effects which determine the formation, stability, and reducing strength of the catalyst Mn(CO)$_3$(α-diimine)(L)•. These three aspects of the ligand dependence are discussed in the next two sections.

Formation and Stability of Mn(CO)$_3$(α-diimine)(L)• Radicals. First of all, processes involving associative reactions between metal radicals and phosphines proceed more rapidly for phosphines having smaller cone angles θ. A smaller cone angle decreases the steric hindrance that hampers the approach of the ligand L to the metal center and consequently facilitates the formation of the radical adduct. For example, the rate at which a CO ligand of Mn(CO)$_5$ is substituted by a phosphine increases dramatically if instead of P(iPr)$_3$ (θ = 160°) the smaller P(nBu)$_3$ (θ = 132°) is used.[45] Steric hindrance also affects the reactions of Mn(CO)$_3$(α-diimine)• radicals. Reaction 4 of **1a**/PR$_3$ mixtures is suppressed for bulky ligands (R = iBu, cHex) but proceeds rapidly for R = nBu, a phosphine with almost the same basicity but with a smaller cone angle.

A measure of the steric hindrance in the approach of the metal atom is the maximum cone angle, θ_{max}, that a phosphine ligand can have to form the radical-phosphine adduct. The IR and UV experiments show that θ_{max} is 140–150° for Mn(CO)$_3$(bpy′)• radicals. Such a value was also reported for the CpMo(CO)$_2$(PR$_3$)• radical[46] but is, of course, much smaller than that of Mn(CO)$_5$• radicals. The formation and stability of Mn(CO)$_3$(α-diimine)(L)• radicals are also determined by electronic effects. The ligand dependence of the Mn(CO)$_3$(α-diimine)(L)• stability is best shown by comparing the reactions of **1a** in the presence of P- and N-donor ligands L. The Mn(CO)$_3$(α-diimine)(L)• radicals would have a higher reducing strength for the more basic N-donor ligands, and this would result in higher yields of reaction 4. In fact, the opposite was observed: high yields were obtained with appropriate phosphines and much lower ones with N-donor ligands. For **1a**/py mixtures it appeared, however, that the disproportionation yield increases at higher pyridine concentrations. The concentration dependence clearly showed that there exists a competition between the processes initiated by Mn(CO)$_3$(α-diimine)• and Mn(CO)$_3$(α-diimine)(L)• radicals. Radical coupling reactions dominate at low Mn(CO)$_3$(α-diimine)(L)• concentrations when the Mn(CO)$_3$(α-diimine)• radicals do not react with L (steric hindrance) or when the stability of the adduct is too low; i.e., when the Mn–L bond is too weak. Because of the strong electron donation of the α-diimine anion, the Mn–L bond is weaker for hard bases such as N- and O-donor ligands than for the less basic phosphines. The above results show that the primary

(40) Andréa, R. R.; de Lange, W. G. J.; Stufkens, D. J.; Oskam, A. *Inorg. Chim. Acta* **1988**, *149*, 77.
(41) tom Dieck, H.; Renk, I. W. *Chem. Ber.* **1971**, *104*, 110.
(42) For Ru(bpy)$_3^{2+}$ and derivatives see: Juris, A.; Balzani, V.; Barigelletti, F.; Campagna, S.; Belser, P.; von Zelewsky, A. *Coord. Chem. Rev.* **1988**, *84*, 85.
(43) Kaim, W.; Olbrich-Deussner, B. In *Organometallic Processes*; Journal of Organometallic Chemistry Library 22; Trogler, W. C., Ed.; Elsevier: Amsterdam, 1990; p 173.
(44) Kaim, W.; Kohlmann, S. *Inorg. Chem.* **1990**, *29*, 2909.
(45) Herrinton, T. R.; Brown, T. L. *J. Am. Chem. Soc.* **1985**, *107*, 5700.
(46) Philbin, C. E.; Goldman, A. S.; Tyler, D. R. *Inorg. Chem.* **1986**, *25*, 4434.

function of L is to form a $Mn(CO)_3(\alpha\text{-diimine})(L)^\bullet$ adduct, which prevents the dimerization of $Mn(CO)_3(\alpha\text{-diimine})^\bullet$ and undergoes the electron-transfer reaction.

Reducing Strength of $Mn(CO)_3(\alpha\text{-diimine})(L)^\bullet$ Radicals. Let us return to the catalytic cycle of the disproportionation of 1, whose mechanism is given in Scheme II. In the two preceding sections we discussed the decomposition of 1 and the formation of the $Mn(CO)_3(\alpha\text{-diimine})(PR_3)^\bullet$ radicals (steps 1 and 2, respectively, of Scheme II). Considering that step 1 is a spontaneous and fast reaction[11,24a,37,39] and provided that L is a small phosphine ligand, then step 3 of Scheme II will be the rate-determining step.

The driving force ΔG of step 3 and other electron-transfer reactions is determined by the redox potentials of the electron donor (D) and acceptor (A). The general expression of ΔG for an electron-transfer reaction

$$D + A \rightarrow D^+ + A^- \qquad (11a)$$

is

$$\Delta G_{(11a)} = -F[E_{1/2}(A/A^-) - E_{1/2}(D^+/D)] \quad (11b)^{47}$$

Unfortunately, eq 11b can not be used for the analysis of electron-transfer reactions that contain irreversible redox couples, since in these cases $E_{1/2}$ is unknown. Kochi showed, however, that peak potentials can be used instead of the reversible half-wave potentials as long as reactions from closely related compounds are compared:

$$\Delta G_{(11a)} = -F[E_{pc}(A) - E_{pa}(D)] + C \qquad (12)$$

(For the derivation and discussion of the exact expression of eq 12, see ref 48). The constant C is eq 12 accounts for the difference between the peak and half-wave potentials. Studies on the coupling reactions of $Mn(CO)_5(PR_3)^+/Mn(CO)_4(PR_3)^-$ and $Co(CO)_3(PR_3)_2^+/Co(CO)_3(PR_3)^-$ ion pairs showed that C is almost independent of the phosphine basicity.[49] Consequently, the difference between the driving forces of two such coupling reactions was calculated from the $E_{pc}(A) - E_{pa}(D)$ values. These differences explained the observed variations in the reactivity of ion pairs.

The same procedure is applied in this article to analyze the α-diimine and phosphine dependence of the electron-transfer reaction (2). In that reaction complex 1 is the electron acceptor A, for which the reduction is irreversible because of the rapid subsequent metal–metal bond splitting, and $Mn(CO)_3(\alpha\text{-diimine})(PR_3)^\bullet$ is the electron donor D. Unfortunately, the radical was too unstable to be investigated. $E_{pa}(D)$ is therefore not accessible, but $E_{pc}(D^+)$ was determined instead by reducing the $Mn(CO)_3(\alpha\text{-diimine})(PR_3)^+$ cation. Adopting eq 12 to the analysis of reaction 2, one obtains

$$\Delta G = -F[E_{pc}(1) - E_{pc}(Mn(CO)_3(\alpha\text{-diimine})(PR_3)^+)] + C' = -F[\Delta E(\alpha\text{-diimine},PR_3)] + C' \qquad (13)$$

The data collected in Table III were used to quantify the phosphine dependence of $\Delta E(\alpha\text{-diimine},PR_3)$ in the case of α-diimine = iPr-DAB. The reduction potentials of $Mn(CO)_3(iPr\text{-}DAB)(PR_3)^+$ shift to more negative potentials for stronger electron-donating phosphines. This phenomenon, previously noticed for many other complexes such as $CpMn(CO)_2(PR_3)$,[26b] $Mn(CO)_5(PR_3)^+$,[26a] and $Co(CO)_3(PR_3)_2^+$,[48b] reflects the extent to which the LUMO of the cation is raised in energy by the σ-donation of the phosphine. As a result, the electron transfer is most favorable for the $P(nBu)_3$-substituted radical (ΔE(iPr-DAB,$P(nBu)_3$) = −0.29 V) and least favorable for the $P(OPh)_3$-substituted one (ΔE(iPr-DAB,$P(OPh)_3$) = −0.49 V). This amounts to a ΔG difference between the $P(nBu)_3$ and $P(OPh)_3$ reactions of 19.3 kJ mol^{-1}.

In addition, the $E_{pc}(Mn(CO)_3(\alpha\text{-diimine})(P(nBu)_3)^+)$ and $E_{pc}(1)$ potentials listed in Table II were used to quantify the α-diimine dependence of $\Delta E(\alpha\text{-diimine},PR_3)$. Both potentials decrease when the $\pi^*(\alpha\text{-diimine})$ orbital energy increases, because the reduction takes place at the α-diimine ligand. $\Delta E(\alpha\text{-diimine},P(nBu)_3)$ is −0.29, −0.16, and −0.13 V for iPr-DAB, iPr-PyCa, and bpy′, respectively. This implies that the electron transfer is most efficient for the bpy′ compounds.

Electron-Transfer Reactions in $1/PR_3/M_3(CO)_{12}$ (M = Fe, Ru) Solutions. Irradiation of $1/PR_3/M_3(CO)_{12}$ (M = Fe, Ru) solutions initiated catalytic reactions of 1 (reaction 4) and of $M_3(CO)_{12-x}(PR_3)_x$ clusters (reaction 6). As we have shown in this paper, both catalyses start with an electron-transfer reaction from the 18-electron $Mn(CO)_3(\alpha\text{-diimine})(PR_3)^\bullet$ radical (reactions 2 and 14, respectively). The mechanism of the catalytic disproportionation of 1 (reaction 4) is shown in Scheme II. The mechanism of the electron-transfer-catalyzed CO substitution of $M_3(CO)_{12}$ is given in Scheme III and was proposed for such reactions of $M_3(CO)_{12}/PR_3$/diphenyl ketone anion (Ph_2CO^-) mixtures.[19,27b] The cluster reaction starts with the reduction of $M_3(CO)_{12}$ (by Ph_2CO^- or, for the systems studied here, by the $Mn(CO)_3(\alpha\text{-diimine})(PR_3)^\bullet$ radical). A carbonyl ligand of the labile $M_3(CO)_{12}^-$ ion is substituted by PR_3, by which the stronger reducer $M_3(CO)_{11}(PR_3)^-$ is formed. $M_3(CO)_{11}(PR_3)^-$ then reduces the parent compound $M_3(CO)_{12}$, thereby closing the catalytic cycle, which is shown in Scheme III.

$$Mn(CO)_3(\alpha\text{-diimine})(PR_3)^\bullet + M_3(CO)_{12} \rightarrow Mn(CO)_3(\alpha\text{-diimine})(PR_3)^+ + M_3(CO)_{12}^- \qquad (14)$$

Scheme III

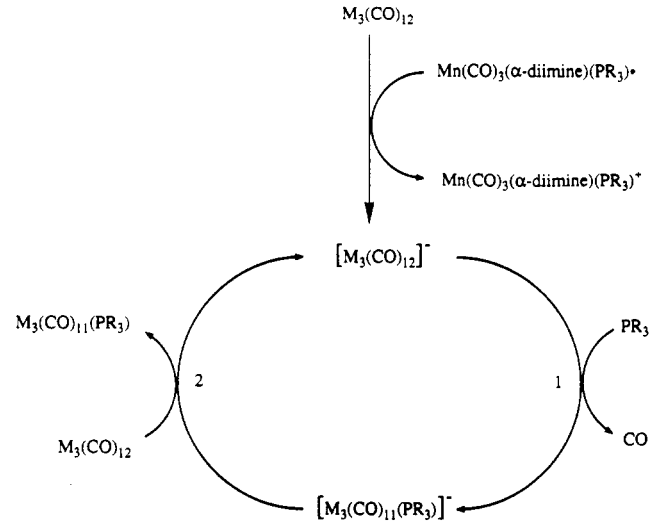

Two one-electron donors, $Mn(CO)_3(\alpha\text{-diimine})(PR_3)^\bullet$ and $M_3(CO)_{11}(PR_3)^-$, are thus formed upon irradiation of $1/PR_3/M_3(CO)_{12}$ solutions. The yield for each of the four possible electron-transfer reactions is determined by their

(47) $E_{1/2} = (E_{pa} + E_{pc})/2$.
(48) (a) Klingler, R. J.; Kochi, J. K. *J. Am. Chem. Soc.* **1980**, *102*, 4790. (b) Klingler, R. J.; Kochi, J. K. *J. Phys. Chem.* **1981**, *85*, 1731.
(49) (a) Lee, K. Y.; Kuchynka, D. J.; Kochi, J. K. *Organometallics* **1987**, *6*, 1866. (b) Lee, K. Y.; Kochi, J. K. *Inorg. Chem.* **1989**, *28*, 567. (c) Kuchynka, D. J.; Kochi, J. K. *Inorg. Chem.* **1989**, *28*, 855.
(50) Servaas, P. C.; Stor, G. J.; Stufkens, D. J.; Oskam, A. *Inorg. Chim. Acta* **1990**, *178*, 185.
(51) The irreversibility refers to the rapid thermal decomposition of the products and not to the electrochemical processes themselves.

driving force and the steric and electronic properties of the phosphine ligand. The influence of the phosphine on the $Mn(CO)_3(\alpha\text{-diimine})(PR_3)^\bullet$ reactions had already been discussed (vide supra). A similar study has not been performed by us for the $M_3(CO)_{11}(PR_3)^-$ radical anions, since it was observed by others that the yield of reaction 6, $x_{(6)}$, is not appreciably affected by the cone angle or basicity of the phosphine.[19] The small influence of the phosphine on $x_{(6)}$ was also determined for the photoreactions of $\mathbf{1a}/PR_3/Ru_3(CO)_{12}$ mixtures (see Table IVb). Reaction 6 is not suppressed in the presence of bulky or weakly basic phosphines (the exceptionally high value of $x_{(6)}/x_{(4)}$ obtained for the $P(cHex)_3$-containing mixture is most probably due to a decrease of $x_{(4)}$). In contrast to this, $x_{(6)}$ strongly depends on the reduction potentials of $M_3(CO)_{12-x}(PR_3)_x$ and 1. Table III shows that the cluster is not substituted at all when it has a reduction potential lower than that of 1.

For M = Fe, the reduction potentials of $M_3(CO)_{12}$ and $M_3(CO)_{11}P(OMe)_3$ are higher than those of the complexes 1 under study. Furthermore, as shown by Table IV, most of the samples yield high values of $x_{(6)}/x_{(4)}$; only for $\mathbf{1b'}$, the α-diimine complex with the highest reduction potential, was a significant disproportionation yield obtained. Obviously $Mn(CO)_3(\alpha\text{-diimine})(PR_3)^\bullet$ reduces $Fe_3(CO)_{12}$ instead of 1, since reaction 14 has a much higher driving force than reaction 2. For M = Ru, the reduction potential of $M_3(CO)_{12}$ lies between those of the compounds 1. The peak differences $E_{pc}(M_3(CO)_{12}) - E_{pc}(1)$ are therefore smaller for M = Ru than for M = Fe. In addition to this, the photochemical activities of the $1/PR_3/Ru_3(CO)_{12}$ samples are not as dominated by reaction 6 as are the corresponding $Fe_3(CO)_{12}$ samples. Again, the electrochemical and photochemical results demonstrate that the yield of the cluster substitution (eq 14) increases in the presence of complexes 1 with lower reduction potentials.

The results of all $1/PR_3/M_3(CO)_{12}$ experiments show that the use of the photogenerated $Mn(CO)_3(\alpha\text{-diimine})(PR_3)^\bullet$ radical as a reducing agent is limited by the presence of the parent complex 1. The reduction of $M_3(CO)_{12}$ by $Mn(CO)_3(\alpha\text{-diimine})(PR_3)^\bullet$ is subdued or even completely suppressed when 1 has a reduction potential lower than that of $M_3(CO)_{12}$. In that case $Mn(CO)_3(\alpha\text{-diimine})(PR_3)^\bullet$ reacts as in the absence of $M_3(CO)_{12}$ by an electron transfer to 1 (reaction 2).

Conclusions

This work describes the reactions of $Mn(CO)_3(\alpha\text{-diimine})(L)^\bullet$ (L = N-, P-donor) radicals. The two catalytic processes that were investigated, the disproportionation of 1 and the CO substitution of $M_3(CO)_{12}$ (M = Fe, Ru), start upon irradiation or reduction of the manganese compounds 1. The reaction cycles of the catalyses contain an electron transfer from the $Mn(CO)_3(\alpha\text{-diimine})(L)^\bullet$ radical to the substrate. The reducing power of the radicals mainly depends on the α-diimine properties and to a lesser extent on the basicity of the ligand L, and this agrees with the fact that the unpaired electron of the $Mn(CO)_3(\alpha\text{-diimine})(L)^\bullet$ radical is located in a $\pi^*(\alpha\text{-diimine})$ orbital. $Mn(CO)_3(\alpha\text{-diimine})(L)^\bullet$ is a less powerful reducer than other, previously studied, metal-centered organometallic radicals. However, an important advantage of these radicals is the high efficiency in which the radical catalyst is formed upon exposition to visible light. This is due to the intense low-energy absorption band of 1 and to the high quantum yield of the corresponding photoreaction ($\Phi \geq 0.4$).[15a,30,33] Further research is under way to optimize the reducing properties of these α-diimine-centered radicals.

Acknowledgment. Mrs. A. M. Roelofsen is thanked for performing the electrochemical measurements and Mr. T. Mahabiersing for the preparation of several compounds. We also thank the Dutch Foundation for Chemical Research (SON) and the Dutch Organization for the Advancement of Pure Research (NWO) for financial support.